Kinetic Characteristics of Phosphofructokinase from Bacillus stearothermophilus: MgATP Nonallosterically Inhibits the Enzyme

ARTICLE *in* BIOCHEMISTRY · APRIL 1994

Impact Factor: 3.02 · DOI: 10.1021/bi00177a036 · Source: PubMed

Kinetic Characteristics of Phosphofructokinase from *Bacillus stearothermophilus*: MgATP Nonallosterically Inhibits the Enzyme†

Malcolm Byrnes, Xiaomao Zhu, Ezzat S. Younathan,* and Simon H. Chang*

Department of Biochemistry, Louisiana State University, Baton Rouge, Louisiana 70803

Received September 28, 1993; Revised Manuscript Received January 6, 1994®

ABSTRACT: The kinetic mechanism of phosphofructokinase from *Bacillus sterothermophilus* has been investigated using steady-state measurements. The double-reciprocal patterns observed for initial velocity, product inhibition, and mixed alternate substrate studies of the reverse reaction establish that the mechanism involves rapid-equilibrium random binding of substrates and the formation of an abortive complex composed of enzyme, MgADP, and fructose 6-phosphate (E–MgADP–Fru-6P). Initial velocity patterns for the forward reaction show significant nonlinearity and resemble those seen for competitive substrate (MgATP) inhibition of an enzyme that obeys a random mechanism. A mutant BsPFK enzyme (GV212) was used to show that the inhibition is not due to MgATP binding in the effector site. Product and dead-end inhibition studies of the forward reaction are consistent with a random mechanism, after taking into account the effects of substrate inhibition by MgATP. Initial velocity measurements at low MgATP concentration show that the binding of MgATP is not a rapid-equilibrium process; i.e., the rate of catalysis is faster than the rate of substrate binding. It is concluded that the kinetic mechanism of the forward reaction is sequential random, with the rate of MgATP binding slower than the catalytic rate. A model is presented that incorporates these results and proposes that substrate binding proceeds through two alternative pathways, one of which is kinetically disfavored. The observed MgATP substrate inhibition arises from both reaction flux through the disfavored pathway and, to some extent, abortive binding of MgATP in the Fru-6P site.

Phosphofructokinase (PFK,[1] EC 2.7.1.11) catalyzes the first committed step of glycolysis, the transfer of a terminal phosphate from ATP to β-D-fructose 6-phosphate (Fru-6P) to form ADP and β-fructose 1,6-bisphosphate (Fru-1,6BP):

$$\text{MgATP} + \text{Fru-6P} \rightarrow \text{MgADP} + \text{Fru-1,6BP}$$

The allosteric PFK from the thermophilic bacterium *Bacillus stearothermophilus*, like its counterpart from *Escherichia coli*, is a tetramer of identical subunits, each composed of 319 amino acids (320 for *E. coli* PFK). Fifty-five percent of the amino acids are identical between the two bacterial enzymes (French & Chang, 1987). Both *B. stearothermophilus* PFK (BsPFK) and *E. coli* PFK (EcPFK) are allosterically inhibited by phosphoenolpyruvate (PEP). This inhibition is reversed by the activators adenosine diphosphate (ADP) and guanosine diphosphate (GDP) (Valdez *et al.*, 1989; Blangy *et al.*, 1968).

A comparison between the crystal structures of BsPFK and EcPFK (Evans *et al.*, 1981; Shirakihara & Evans, 1988) reveals striking structural similarity. The two enzymes have all the same secondary structural elements, and their subunit α-carbon traces are nearly superimposable. In both enzymes, the subunit is divided into a large and a small domain, with the active site located within the subunit in a cleft between the two domains. The active-site residues that bind substrates are either the same or similar between the two enzymes.

Despite the high degree of structural similarity between BsPFK and EcPFK, there is a significant kinetic difference between them. Steady-state initial velocity studies reveal that whereas saturation of EcPFK by Fru-6P is highly cooperative in the presence of saturating MgATP (Blangy *et al.*, 1968), saturation of BsPFK by Fru-6P shows little or no cooperativity under the same conditions (Valdez *et al.*, 1989). Fructose 6-phosphate saturation of BsPFK is cooperative, however, in the presence of PEP (Valdez *et al.*, 1989). Thus, BsPFK resembles the PFK from the extreme thermophilic bacterium *Flavobacterium thermophilum* (Yoshida, 1972), which likewise displays a hyperbolic Fru-6P saturation profile that become sigmoidal in the presence of PEP. Schirmer and Evans (1990) have proposed a structural model for the allosteric transition of BsPFK based on X-ray diffraction data.

Although the structure of BsPFK has been extensively investigated, its kinetic characteristics have remained largely unstudied. For example, although the amino acid residues involved in binding the substrates MgATP and Fru-6P have been known for some time (Evans *et al.*, 1981), the kinetic mechanism has not been studied. Several observations suggest that there are differences between the active-site regions of BsPFK and EcPFK; (i) the active-site structure of BsPFK is more open than that of EcPFK (Shirakihara & Evans, 1988), (ii) significant binding of GDP occurs in the active site of BsPFK (Valdez *et al.*, 1989) but not in the active site of EcPFK (Blangy *et al.*, 1968), and (iii) the large (ATP-binding) domain of EcPFK moves as the enzyme changes conformation from a "closed" to an "open" subunit structure (Shirakihara & Evans, 1988), whereas the large domain of BsPFK remains essentially rigid during the allosteric transition of the enzyme (Schirmer & Evans, 1990).

These observations have stimulated our interest in studying the kinetic characteristics of the BsPFK-catalyzed reaction in both the forward and reverse directions. Initial velocity, product inhibition, and mixed alternate substrate studies of the reverse reaction indicate that the kinetic mechanism is

† Supported by National Institutes of Health Grant DK31676.

* Authors to whom correspondence should be addressed.

® Abstract published in *Advance ACS Abstracts*, March 1, 1994.

[1] Abbreviations: PFK, phosphofructokinase; BsPFK and EcPFK, the phosphofructokinases from *Bacillus stearothermophilus* and *Escherichia coli*, respectively; GV212, mutant *B. stearothermophilus* phosphofructokinase with glycine 212 mutated to valine; *bspfk*, the *B. stearothermophilus* phosphofructokinase gene; Fru-6P, fructose 6-phosphate; Fru-1,6BP, fructose 1,6-bisphosphate; PEP, phosphoenolpyruvate; Ara-5P, arabinose 5-phosphate; AMPPCP, β,γ-methyleneadenosine 5′-triphosphate; AMPPNP, adenylyl imidodiphosphate; SDS, sodium dodecyl sulfate.

0006-2960/94/0433-3424$04.50/0

sequential random. Product and dead-end inhibition studies of the forward reaction corroborate this result. However, initial velocity studies of the forward reaction indicate that MgATP is a nonallosteric substrate inhibitor, and the binding of MgATP is a non-rapid equilibrium process. On the basis of these results, it is proposed that substrate binding proceeds via two alternative steady-state pathways, with one pathway kinetically favored over the other. Substrate inhibition by MgATP is proposed to result from both abortive binding of MgATP in the Fru-6P site and reaction flux through the disfavored pathway.

MATERIALS AND METHODS

Enzymes and Chemicals. NADH, $NADP^+$, Fru-6P, ATP, Fru-1,6BP, ADP, PEP, Ara-5P, AMPPCP, and the auxiliary enzymes for the coupled PFK activity assays were all obtained from Sigma Chemical Co. (St. Louis, MO). The Cibacron Blue 3GA–agarose (Type 3000-CL-L) resin was also obtained from Sigma. Restriction endonucleases used for cloning were obtained from either New England Biolabs (Beverly, MA) or U.S. Biochemical (Cleveland, OH).

Expression and Purification of PFK. BsPFK was expressed in PFK-deficient *E. coli* cells (DF1020 cells) from a recombinant plasmid constructed by cloning the *bspfk* gene (French & Chang, 1987) into the *Eco*RI/*Hin*dIII sites of pUC18. The enzyme was subsequently purified by a three-step procedure (Valdez *et al.*, 1989) involving (1) sonication, (2) heat treatment at 70 °C, and (3) chromatography on a Cibacron Blue 3GA affinity column. The purified enzyme preparation had a specific activity of 160 units/mg. Its purity was demonstrated by the presence of a single band on an SDS–polyacrylamide gel stained with Coomassie Brilliant Blue dye. The purified enzyme solution was dialyzed at 4 °C in 100 mM Tris-HCl, pH 7.4, containing 1 mM dithiothreitol and 50% glycerol, and stored at −20 °C. Protein concentration was determined using the Bio-Rad (Richmond, CA) protein assay.

Site-Directed Mutagenesis and Expression and Purification of Mutant BsPFK. The site-directed mutagenesis procedure to mutate the *bspfk* gene, as well as the procedures for expression and purification of the mutant enzyme, are to be described separately (Zhu *et al.*, manuscript in preparation).

Kinetic Assays. The initial velocity of the PFK-catalyzed reaction in the forward direction was measured at 30 °C[2] in 100 mM Tris-HCl, pH 8.2, containing 10 mM $MgCl_2$ and 5 mM NH_4Cl by coupling the production of either Fru-1,6BP or ADP to the oxidation of NADH (0.20 mM). The Fru-1,6BP-coupled assay utilized the auxiliary enzymes aldolase (20 μg/mL), triosephosphate isomerase (10 μg/mL), and α-glycerophosphate dehydrogenase (10 μg/mL), while the ADP-coupled assay utilized pyruvate kinase (10 μg/mL), phosphoenolpyruvate (PEP, 200 μM) and lactate dehydrogenase (10 μg/mL). The ADP-coupled assay system could not be used for Fru-6P saturation studies since PEP is an allosteric inhibitor with respect to Fru-6P; however, PEP at this concentration (200 μM) does not alter MgATP saturation behavior. The ATP-regenerating system that utilizes creatine kinase and creatine phosphate, which is required for the EcPFK activity assay, was found to be unnecessary since ADP has little or no activating effect on BsPFK (in the absence of PEP). In all forward reaction assays, the free Mg^{2+} concentration was kept 5–10 mM in excess of the ATP concentration to avoid inhibition by free ATP. Typically, assays were initiated by the addition of 0.10 μg of PFK. Since the BsPFK assay generally involved an initial nonlinear phase, a 1- or 2-min lag period was allowed prior to recording the Abs_{340} change over time, which was done for at least 1 min. A thermostated Hitachi UV-2000 spectrophotometer was used for these measurements. Duplicate assays were run for each data point. Initial velocities are expressed in units of micromoles of product formed per minute.

Initial velocity measurements in the reverse direction were similar to those in the forward direction, except that the production of either Fru-6P or ATP was coupled to the reduction of $NADP^+$ (0.20 mM). Assays were run at pH 8.2, and Mg^{2+} concentration was kept 9–10 mM in excess of the ADP concentration. For the Fru-6P-coupled assay, the auxiliary enzymes phosphoglucoisomerase (10 μg/mL) and glucose-6-phosphate dehydrogenase (10 μg/mL) were used, whereas for the ATP-coupled assay, hexokinase (20 μg/mL), glucose (3 mM), and glucose-6-phosphate dehydrogenase (10 μg/mL) were used. Typically, assays were initiated with the addition of 2.0 μg of PFK.

Treatment of Kinetic Data. Initial velocity data for the forward reaction were fit to either the Michaelis–Menten equation (eq 1), the Hill equation (eq 2), the initial velocity equation for a rapid-equilibrium sequential mechanism (eq 3; Cleland, 1963), or the initial velocity equation for a sequential random mechanism assuming steady-state (non-rapid-equilibrium) conditions (eq 4; Ferdinand, 1966). In eqs 1–7, [A] and [B] represent the concentrations of substrates A and B, and V_{max} is the maximum velocity. In eq 1, K_m is the Michaelis constant, whereas in eq 2, $[A]_{1/2}$ is the concentration of substrate at half-saturation and n is the Hill coefficient. In eq 3, K_{ia} is the equilibrium constant for dissociation of substrate A from the binary complex EA (E represents enzyme). There is an analogous constant, K_{ib}, for dissociation of B from EB. K_a and K_b are equilibrium constants for dissociation of A and B, respectively, from the ternary complex EAB. In eq 4, the terms i, j, k, l, and m are complex functions of [B] and the rate constants for the various steps in Scheme 1 (see Discussion section). As such, i–m have no physical significance.

$$v = \frac{V_{max}[A]}{[A] + K_m} \quad (1)$$

$$v = \frac{V_{max}[A]^n}{[A]_{1/2} + [A]^n} \quad (2)$$

$$v = \frac{V_{max}[A][B]}{K_{ia}K_b + K_b[A] + K_a[B] + [A][B]} \quad (3)$$

$$v = \frac{i[A]^2 + j[A]}{k + l[A]^2 + m[A]} \quad (4)$$

Initial velocity data for product inhibition, dead-end inhibition, and alternate substrate studies were first plotted graphically as double-reciprocal plots. On the basis of these primary plots, the inhibition patterns were identified, and each data set was fit to the equation for either linear competitive (eq 5), linear noncompetitive (eq 6), or linear uncompetitive (eq 7) inhibition (Cleland, 1979). In eqs 5–7, the constant K is the equilibrium constant for dissociation of varied substrate A from the ternary complex EAB, whereas K_{is} and K_{ii} are equilibrium constants for dissociation of inhibitor I from its

[2] The saturation curves with respect to substrates Fru-6P and MgATP obtained at 30 °C were similar to those obtained at 60 °C, except that the k_{cat} was lower at 30 °C. Fru-6P saturation was noncooperative at both temperatures, and substrate inhibition was apparent with high [MgATP] at both temperatures.

inhibitory complex, as determined from slope and intercept replots, respectively. All curve-fitting to eqs 1–7 was per-

$$v = \frac{V_{max}[A]}{K(1 + [I]/K_{is}) + [A]} \quad (5)$$

$$v = \frac{V_{max}[A]}{K(1 + [I]/K_{is}) + [A](1 + [I]/K_{ii})} \quad (6)$$

$$v = \frac{V_{max}[A]}{K + [A](1 + [I]/K_{ii})} \quad (7)$$

formed by nonlinear regression analysis using the program INPLOT (GraphPad, Inc., San Diego, CA).

RESULTS

The Reverse Reaction: Initial Velocity, Product Inhibition, and Mixed Alternate Substrate Studies. Because the kinetic behavior of BsPFK in the forward direction is more complex than in the reverse direction, studies on the latter are presented first. The turnover number k_{cat} of the reverse reaction (3.2 s^{-1}) was about 35-fold lower than that of the forward reaction (112 s^{-1}). This compare well to the 40-fold lower value for the reverse reaction of EcPFK relative to its forward reaction (Hellinga & Evans, 1987).

Initial velocity studies were performed on the reverse reaction by varying Fru-1,6BP concentration while keeping MgADP concentration constant at different fixed levels, and vice versa. Double-reciprocal plots were constructed for both sets of data. The families of lines obtained for both (Figure 1) intersect to the left of the ordinate, a result which denotes a sequential kinetic mechanism. The initial velocity data were fit to the equation for a rapid-equilibrium random or ordered bireactant mechanism (eq 3), assuming that A is MgADP and B is Fru-1,6BP. The following parameters were obtained by performing nonlinear regression analysis of the initial velocity data (Cleland, 1979) using eq (3): k_{cat} = 3.2 ± 0.2 s^{-1}, K_a = 0.11 ± 0.01 mM, K_b = 0.44 ± 0.05 mM, K_{ia} = 0.33 ± 0.04 mM, and K_{ib} = 0.19 ± 0.08 mM.

Product inhibition studies were also performed on the reverse reaction to further distinguish whether its mechanism is random or ordered. For these studies, the concentration of one substrate (Fru-1,6BP or MgADP) was varied while the other was kept constant at a fixed level in the absence or presence of different amounts of one of the two products (Fru-6P or MgATP). Four sets of product inhibition data were obtained. The data from each inhibition study were fit to the equation for either linear competitive (eq 5), linear noncompetitive (eq 6), or linear uncompetitive (eq 7) inhibition. Table 1 lists the pertinent kinetic parameters obtained and the patterns of lines observed in double-reciprocal plots. The results are consistent with a rapid-equilibrium random mechanism in the reverse direction. The noncompetitive product inhibition by Fru-6P with respect to MgADP indicates the formation of a dead-end E–MgADP–Fru-6P complex. However, the equations for both competitive and noncompetitive inhibition fit equally well to the data for inhibition by MgATP with respect to Fru-1,6BP, a result which indicates that the dead-end E–MgATP–Fru-1,6BP complex probably does not form readily, if it forms at all.

Additional evidence that the mechanism in the reverse direction is random was obtained from studies using GDP, which can function as an alternate substrate for the reverse reaction. When GDP is added to a PFK assay in which

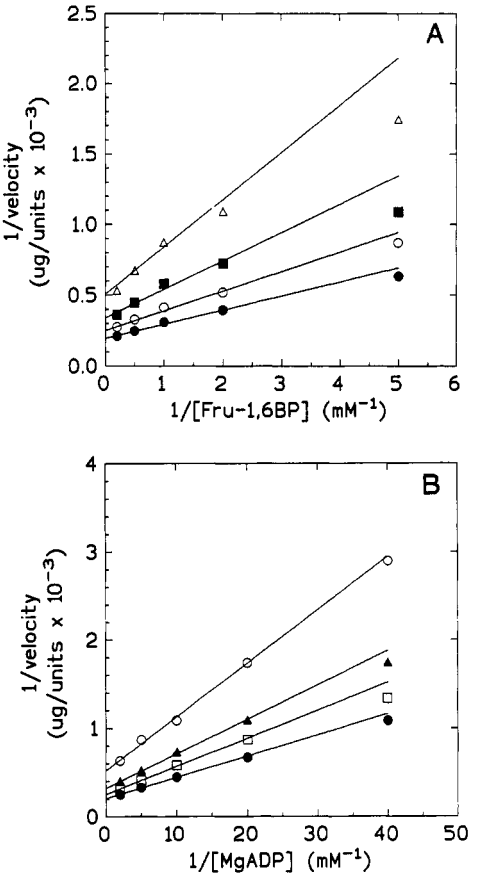

FIGURE 1: Initial velocity patterns for the reverse reaction. (A) Plot of the reciprocal of initial velocity *versus* the reciprocal of Fru-1,6BP concentration at different fixed levels of MgADP: (▲) 0.05 mM, (■), 0.10 mM, (○) 0.20 mM, and (●) 0.5 mM MgADP. (B) Plot of the reciprocal of initial velocity *versus* the reciprocal of MgADP concentration at different fixed levels of Fru-1,6BP: (○) 0.20 mM, (▲) 0.50 mM, (□) 1.0 mM, and (●) 2.0 mM. The lines were drawn using linear equations containing parameters generated from direct curve-fitting to eq 3. Initial velocities (units per microgram) were measured using the Fru-6P-coupled assay.

Table 1: Product Inhibition Patterns for the Reverse Reaction

[Fru-1,6BP] (mM)	[MgADP] (mM)	inhibitor	pattern[a]	K_{is} (μM)	K_{ii} (μM)
varied	0.91	MgATP[b]	NC (or C)	52 ± 4	676 ± 47
0.50	varied	MgATP	C	14 ± 1	na
0.50	varied	Fru-6P[c]	NC	7 ± 2	55 ± 11
varied	0.91	Fru-6P	C	6 ± 0.5	na

[a] NC = noncompetitive; C = competitive inhibition. [b] When MgATP was the product inhibitor, the Fru-6P-coupled assay was used. [c] When Fru-6P was the product inhibitor, the ATP-coupled assay was used. na, not applicable.

$NADP^+$ reduction is coupled to ATP *via* hexokinase (see Materials and Methods section), which will not accept GTP as a substrate, the GTP produced in the reverse PFK reaction is not detected and "inhibition" results. The curvature or linearity of double-reciprocal plots for initial velocity studies in the presence of GDP can provide evidence as to whether the mechanism is ordered, with ADP (GDP) binding first (curved plots), or random (linear plots). As expected, the plots obtained showed that GDP is a competitive "inhibitor" with respect to MgADP and a noncompetitive "inhibitor" with respect to Fru-1,6BP, indicating that ADP (or GDP) can bind first to the enzyme in either an ordered or a random mechanism. More significantly, the plots were linear. This result is consistent with a random mechanism, since nonlinear inhibition would have been observed had the mechanism been ordered.

A similar result has been reported for rabbit muscle PFK (Hanson *et al.*, 1973). Altogether, the results of both the product inhibition and the mixed alternate substrate studies in the reverse direction are consistent with a rapid-equilibrium random mechanism that includes the formation of an abortive E–MgADP–Fru-1,6P complex.

The Forward Reaction: Fructose 6-Phosphate Saturation of BsPFK. Valdez *et al.* (1989) showed that Fru-6P saturation of BsPFK is hyperbolic. Our findings confirm this result and further indicate that simple Michaelis–Menten kinetics cannot fully explain the saturation behavior of BsPFK. As shown in Figure 2A (dashed curve), in the presence of varied Fru-6P concentrations that are less than about one-third the fixed MgATP concentration, the Fru-6P saturation data fit the Michaelis–Menten equation well ($R^2 = 0.994$). A K_m(Fru-6P) of 0.03 mM is obtained under these conditions. However, when the [Fru-6P]/[MgATP] ratio is greater than about 1/3 (Figure 2A, upper curve), a flattening is observed. Thus, when analyzed over the entire 0.01–1.0 mM range, the saturation data fit the Michaelis–Menten equation less well ($R^2 = 0.988$).

In the presence of high levels of MgATP (greater than $30K_m$) Fru-6P saturation curves do not flatten within the normal 0.01–1.0 mM Fru-6P concentration range. Rather, saturation follows Michaelis–Menten kinetics (Figure 2A, lower curve) throughout the entire range. Inhibition by MgATP is apparent, and this inhibition appears competitive with respect to Fru-6P (Figure 2A, inset). Indeed, when Fru-6P saturation data collected in the presence of fixed levels of MgATP equal to 0.5 mM, 5.0 mM, and 10.0 mM are analyzed according to the method of Cleland (1979), the data fit the equation for linear competitive inhibition (eq 5) well, yielding a linear slope replot and a K_{is} of 5.2 ± 0.5 mM. A Hill coefficient of 1.05 ± 0.05 is obtained for each of the three saturation curves. Thus, MgATP inhibition is not associated with cooperative Fru-6P binding as it is for EcPFK, where Hill coefficients increase from 1.4 to 3.6 in the presence of fixed MgATP concentrations ranging from very low levels to above-saturating levels (Johnson & Reinhart, 1992).

The flattening effect observed in the Fru-6P saturation curve when the [Fru-6P]/[MgATP] ratio is greater than about 1/3 is seen in double-reciprocal plots as a leveling-off of the slope near the $1/v$ axis. This leveling-off effect is evident in Figure 2B, which shows initial velocity plots with respect to variable Fru-6P concentration at different fixed levels of MgATP near its K_m value. These results indicate that MgATP concentration is rate-limiting when the [MgATP]/[Fru-6P] ratio is less than 2 or 3. The effect is more apparent in Figure 2C, which shows that the reaction rate remains steady and independent of Fru-6P concentration between 0.033 and 5.0 mM in the presence of fixed MgATP concentrations at or below its K_m value (0.1 mM). Overall, these studies suggest that MgATP binds to BsPFK under non-rapid-equilibrium conditions and that the rate of catalysis is faster than the rate of MgATP binding. [The deviation from linearity at low Fru-6P concentration in the presence of 0.1 and 0.2 mM MgATP in Figure 2B is most likely the result of substrate binding via a kinetically disfavored pathway (see Discussion section).]

The linear regions of the plots in Figure 2B can be fit to the initial velocity equation for a sequential bireactant mechanism in rapid equilibrium (eq 3), assuming A is MgATP and B is Fru-6P. When this is done, the following kinetic parameters are obtained: $k_{cat} = 112 \pm 7\ s^{-1}$, $K_a = 40 \pm 27\ \mu M$, $K_b = 2 \pm 18\ \mu M$, and $K_{ib} = 68 \pm 43\ \mu M$. The double-reciprocal lines generated from curve-fitting to eq 3 intersect to the left of the ordinate and on the abscissa, a result consistent with a sequential mechanism in the forward direction.

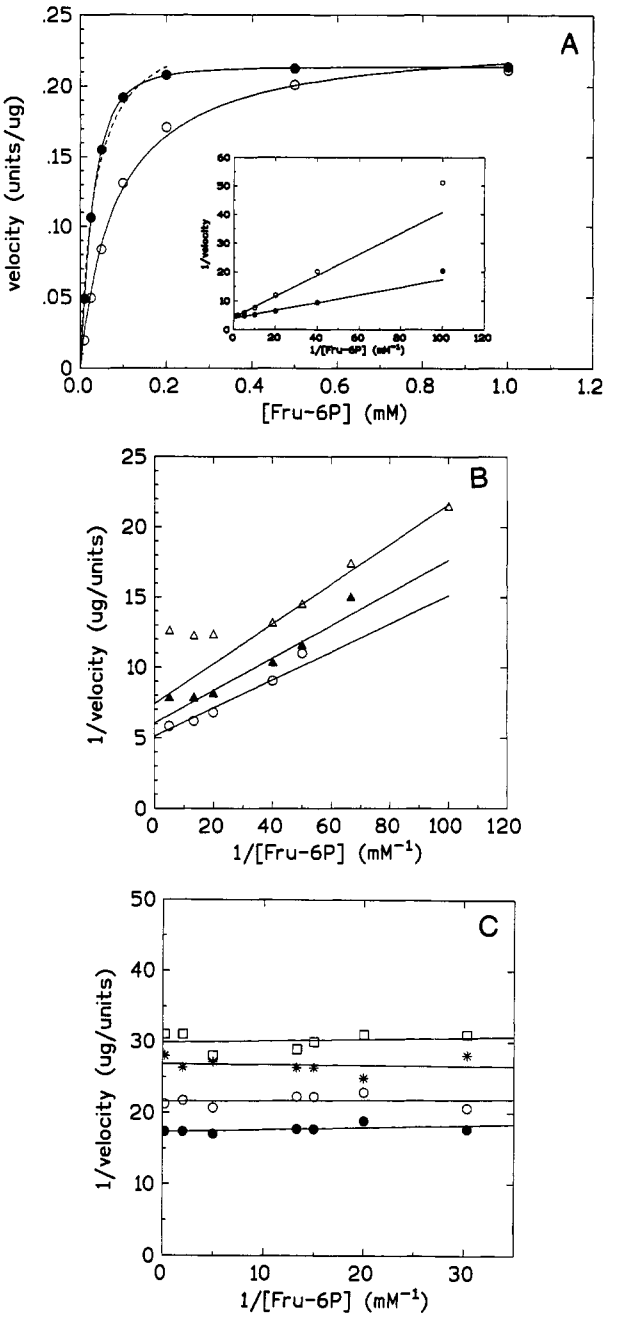

FIGURE 2: (A) Fru-6P saturation curves. Dependence of the velocity of the BsPFK-catalyzed reaction on Fru-6P concentration in the presence of (●) 0.5 mM or (○) 10.0 mM MgATP is shown. The upper curve was generated by fitting the data to eq 4, whereas the lower curve was generated by curve-fitting to eq 1. The dashed line was generated by fitting the data between 0.01 and 0.2 mM Fru-6P in the upper curve to eq 1. (Inset) Double-reciprocal plots of the same data. The lines were drawn using linear equations containing parameters generated from fitting the data between 0.01 and 0.2 mM Fru-6P to eq 1. Initial velocities (units per microgram) were measured using the Fru-1,6BP-coupled assay. (B) Initial velocity plot. Reciprocal of initial velocity *versus* reciprocal of Fru-6P concentration between 0.01 and 0.20 mM Fru-6P in the presence of (△) 0.05, (▲) 0.10, and (○) 0.20 mM MgATP. The lines were drawn using linear equations containing parameters generated by direct fitting of a selected range of data points to eq 3. (C) Initial velocity plot. Reciprocal of initial velocity *versus* reciprocal of Fru-6P concentration between 0.033 and 5.0 mM Fru-6P in the presence of different fixed low levels of MgATP: (□) 0.04 mM, (*) 0.05 mM, (○) 0.067 mM, and (●) 0.10 mM. Lines were generated by linear regression analysis.

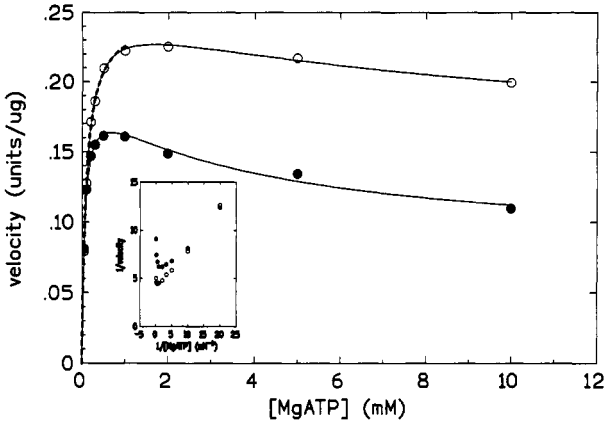

FIGURE 3: Dependence of the BsPFK-catalyzed reaction rate on MgATP concentration. Fru-6P concentration was kept fixed at (●) 0.05 mM or (○) 0.2 mM. Both curves were generated by fitting the data to eq 4. The thick dashed line was generated by fitting the data between 0.05 and 1.0 mM in the upper curve to eq 1. (Inset) Double-reciprocal plots of the same data.

MgATP Saturation and Substrate Inhibition. The Michaelis–Menten equation fits the MgATP saturation data well ($R^2 = 0.996$) in the presence of saturating Fru-6P as long as the varied MgATP concentration is below 10-fold the fixed Fru-6P concentration (Figure 3, thick dashed line). A K_m(MgATP) of 0.1 mM is obtained under these conditions. However, inhibition becomes apparent at high MgATP concentrations (Figure 3, both curves), and this inhibition is more pronounced at the lower Fru-6P concentration (lower curve). Furthermore, as the fixed level of Fru-6P is decreased, the inhibition becomes apparent at a lower MgATP concentration. The saturation curves tend to rise to a maximum and then decrease to a plateau.

The inhibition by high levels of MgATP results in nonlinear double-reciprocal plots with respect to variable MgATP concentration. As shown in Figure 3 (inset), the double-reciprocal plots pass through a minimum and then bend upward as they approach the $1/v$ axis. This initial velocity pattern is indicative of substrate inhibition (Segel, 1975a) by high levels of MgATP. Because of their upward curvature, the lines do not intersect to the left of the ordinate. Thus, the initial velocity data with respect to MgATP do not fit the equation for a sequential bireactant mechanism in rapid equilibrium (eq 3).

MgATP Saturation of the GV212 BsPFK Mutant. It is conceivable that the inhibition exhibited by MgATP results from the binding of MgATP in a site other than the active site, e.g., the effector site. In order to address this possibility, the ability of MgATP to inhibit a mutant BsPFK enzyme that has the glycine at position 212 replaced with a valine (GV212) was investigated. Glycine 212 is located at the hinge of the 8H loop, which has been proposed to be important in the BsPFK allosteric transition (Schirmer & Evans, 1990). Residue 212 is situated along the border of the effector binding cleft near the site where the purine ring of a bound ADP or GDP molecule would be located.

We have found that PEP inhibition of the GV212 mutant cannot be reversed by GDP or ADP and that neither ADP nor GDP bind well to the effector site (Zhu *et al.*, manuscript in preparation). Presumably, binding of MgATP in the effector site would likewise be disrupted. Figure 4 shows that the ability of MgATP to inhibit the enzyme is unaffected by the mutation (the curves appear nearly identical). This observation suggests that the inhibition is not due to the binding of MgATP in the effector site.

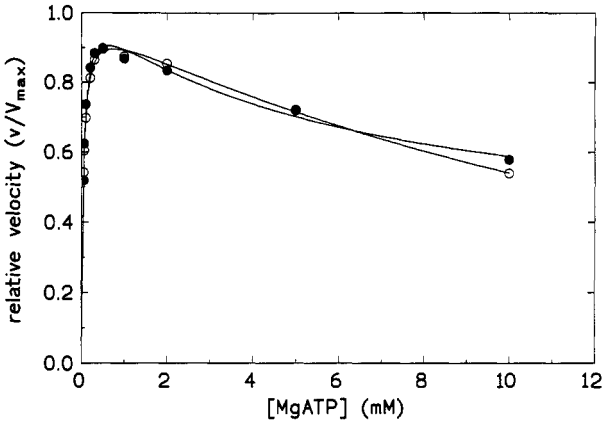

FIGURE 4: MgATP inhibition of the mutant GV212 BsPFK enzyme. Initial velocity was measured *versus* MgATP concentration for (●) mutant and (○) wild-type BsPFK in the presence of 0.05 mM Fru-6P. Both curves were generated by curve-fitting to eq 4.

Table 2: Alternative Nucleoside Triphosphate Substrates

NTP	K_m(NTP)[a] (mM)	% of k_{cat}(ATP)	K_m(Fru-6P)[b] (μM)
ATP	0.07 ± 0.01	100	33 ± 5
GTP	0.18 ± 0.01	73	28 ± 4
CTP	2.6 ± 0.2	98	146 ± 19
UTP	2.8 ± 0.2	93	68 ± 7

[a] Fru-6P concentration was kept fixed at 1.0 mM (saturating) for these determinations. [b] NTP concentration was kept fixed at 5K_m(NTP). In each assay, Mg^{2+} was present in excess of the NTP concentration.

Alternative Nucleoside Triphosphate (NTP) Substrates. In addition to ATP, the nucleoside triphosphates GTP, UTP, and CTP can all serve as phosphate donors in the BsPFK-catalyzed reaction. All four NTPs display saturation profiles similar to those in Figure 3, which tend to rise to a maximum and then drop to a plateau at high MgNTP concentrations. Surprisingly, although the four NTPs have different Michaelis constants (Table 2), they all give the same relative velocity (v/V_{max}) at a concentration of 10 mM (not shown). Thus, they inhibit BsPFK to essentially the same extent when present at high (10 mM) concentration.

Product and Dead-End Inhibition Studies of the Forward Reaction. Product inhibition studies as well as dead-end inhibition studies using the nonreactive ATP analogs β,γ-methyleneadenosine 5′-triphosphate (AMPPCP) and 5′-adenylyl imidodiphosphate (AMPPNP) and the nonreactive Fru-6P analog arabinose 5-phosphate (Ara-5P), were performed on the forward reaction in order to further delineate the kinetic mechanism. As with the reverse reaction, primary double-reciprocal plots were constructed to determine the nature of the inhibition, and the saturation data were fit directly to equations for linear competitive, linear noncompetitive, and linear uncompetitive inhibition. The patterns obtained in the plots and the parameters obtained from curve-fitting are shown in Table 3.

The product and dead-end inhibition results for the forward reaction are somewhat more difficult to interpret than are the product inhibition results for the reverse reaction. The double-reciprocal plots for inhibition by both Fru-1,6BP and Ara-5P with respect to MgATP (up to 1 mM) yield nearly parallel yet divergent lines (Table 3). In both of these inhibition studies, when the MgATP concentration is extended to 10 mM, the plots bend upward as they approach the $1/v$ axis, indicating substrate inhibition at high (>2 mM) MgATP concentration. Because of the curvature, it is not possible from these plots alone to establish whether the inhibition is

Table 3: Product and Dead-End Inhibition Patterns for the Forward Reaction

(A) Product Inhibition Patterns

[Fru-6P] (mM)	[MgATP] (mM)	product inhibitor	pattern[a]	K_{is} (mM)	K_{ii} (mM)
0.2	varied	MgADP	C	0.503 ± 0.006	na
varied	0.87	MgADP[b]	NC	22 ± 2	3.92 ± 0.05
1.0	varied	Fru-1,6BP[c]	UC (NC)[d]	na	14 ± 2

(B) Dead-End Inhibition Patterns[b]

[Fru-6P] (mM)	[MgATP] (mM)	dead-end inhibitor	pattern	K_{is} (mM)	K_{ii} (mM)
0.20	varied	AMPPCP	C	1.12 ± 0.04	na
varied	0.87	AMPPCP	NC	10.2 ± 0.9	9.8 ± 0.8
0.20	varied	AMPPNP	C (or NC)	0.05 ± 0.02	1.56 ± 0.81
varied	0.87	AMPPNP	NC	0.29 ± 0.09	0.40 ± 0.12
varied	0.87	Ara-5P	C	1.2 ± 0.2	na
0.20	varied	Ara-5P	UC (NC)[d]	na	6.2 ± 0.5

[a] NC = noncompetitive, C = competitive, and UC = uncompetitive. [b] The Fru-1,6BP-coupled assay was used for these studies. [c] When Fru-1,6BP was the product inhibitor, the ADP-coupled assay system was used. Fru-1,6BP inhibition with respect to Fru-6P could not be determined since the phosphoenolpyruvate required for the assay is an allosteric inhibitor of BsPFK at low Fru-6P concentration. [d] Parallel lines were observed in the double-reciprocal plots. See the text for further discussion. The pattern in parentheses is that expected in the absence of substrate inhibition. na, not applicable.

uncompetitive (parallel lines) or noncompetitive (convergent lines). An uncompetitive inhibition pattern would be expected in these studies if the kinetic mechanism were ordered with MgATP binding first, whereas a noncompetitive pattern would be expected if the mechanism were random. However, the ordered mechanism under consideration here is incompatible with the competitive nature of the inhibition by MgATP with respect to Fru-6P seen in Figure 2A. Competitive substrate inhibition by MgATP would be possible for an ordered mechanism only when Fru-6P is the first substrate to bind to the enzyme; it is not possible for an ordered mechanism in which MgATP binds first to the enzyme (Segel, 1975a). On the other hand, competitive substrate inhibition by MgATP with respect to Fru-6P is consistent with a random mechanism. In this case, inhibition can occur in several ways, including the two being proposed here: (1) abortive binding of MgATP in the Fru-6P site and (2) reaction flux through a kinetically disfavored substrate binding pathway (see below). Thus, taking the substrate inhibition into account, the most likely interpretation of the product and dead-end inhibition results is that Fru-6P and MgATP bind to the enzyme in random order.

An examination of the AMPPCP and AMPPNP inhibition patterns (Table 3) sheds light on the mechanism by which ATP inhibits BsPFK. Although AMPPCP inhibition with respect to ATP is purely competitive, AMPPNP inhibition with respect to ATP, though mostly competitive, nevertheless has some noncompetitive character. In the latter case, the lines in the double-reciprocal plot (Figure 5A) clearly converge just to the left of the $1/v$ axis. The simplest interpretation of this result is that AMPPNP (and presumably ATP) binds abortively in the Fru-6P site, forming a dead-end E–MgATP–AMPPNP [or E–$(MgATP)_2$] complex. Further evidence for the formation of this complex is seen in the double-reciprocal plot for AMPPNP inhibition with respect to Fru-6P (Figure 5B), which gives an essentially noncompetitive (mixed-type) pattern composed of lines that interest progressively closer to the $1/v$ axis as AMPPNP concentration is increased. This effect is not seen for AMPPCP. AMPPCP apparently does not bind abortively as does AMPPNP, most likely because the orientation of its γ-phosphate group is quite different from

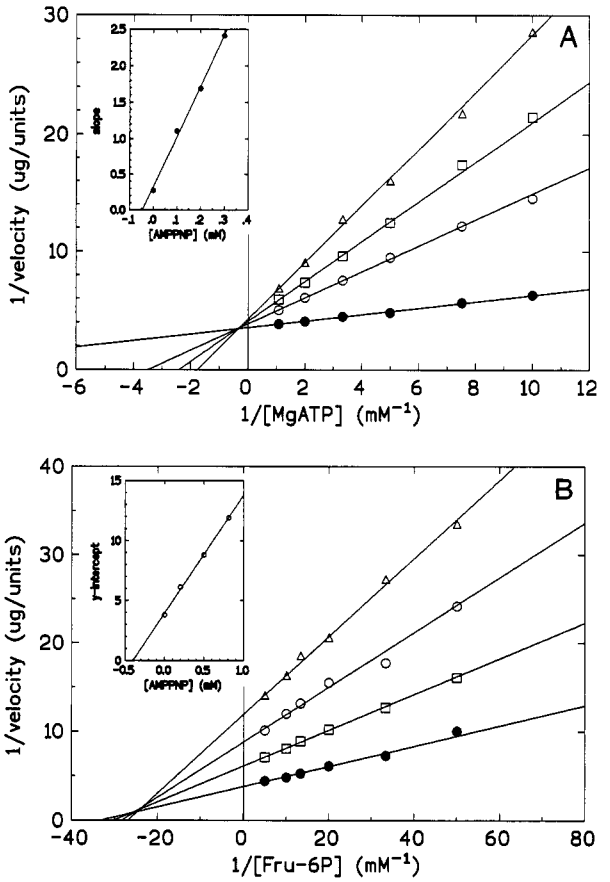

FIGURE 5: AMPPNP inhibition patterns. (A) Plot of the reciprocal of initial velocity *versus* the reciprocal of MgATP concentration in the presence of 0.2 mM Fru-6P and (●) 0 mM, (○) 0.1 mM, (□) 0.2 mM, or (△) 0.3 mM AMPPNP. (Inset) Slope replot. (B) Plot of the reciprocal of initial velocity *versus* the reciprocal of Fru-6P concentration in the presence of 0.87 mM MgATP and (●) 0 mM, (□) 0.2 mM, (○) 0.5 mM, or (△) 0.81 mM AMPPNP. (Inset) Intercept replot. Initial velocities (units per microgram) were measured using the Fru-1,6BP-coupled assay.

that of AMPPNP, which is similar to that of ATP (Yount *et al.*, 1971; Larsen *et al.*, 1969). These results suggest that ATP binds in the Fru-6P site *via* its γ-phosphate group. Thus, abortive binding at least partially explains the inhibition seen at high MgATP concentration.

DISCUSSION

The intersecting patterns of lines obtained in the double-reciprocal initial velocity plots for the reverse reaction indicate that the kinetic mechanism is sequential rather than ping-pong. Further, the patterns of lines obtained in the reverse reaction product inhibition (Table 1) and mixed alternate substrate (GDP) studies indicate that the kinetic mechanism of the reverse reaction is rapid equilibrium random. The results of product inhibition and dead-end inhibition studies of the forward reaction (Table 3) are also consistent with a random mechanism, after taking into account the effect of substrate inhibition by MgATP. The binding of MgATP to the enzyme was found to be rate-limiting when its concentration is low. Thus, the kinetic mechanism of BsPFK in the forward direction can best be described as sequential random with binding of MgATP being rate-limiting, i.e., the rate of its binding is lower than the catalytic rate. The kinetic mechanism in the forward direction is depicted in Scheme 1, where E is free enzyme, A and B are substrates MgATP and Fru-6P, respectively, E–A and E–B are their binary complexes, and

Scheme 1

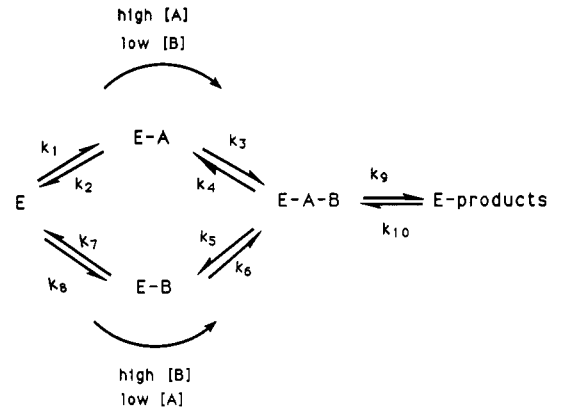

E–A–B is the reactive, ternary complex. The constants k_1–k_{10} are rate constants for the steps indicated. It is assumed that the binding of MgATP is slow relative to the catalytic step, i.e., $k_1, k_6 \ll k_9$. The curved arrows in Scheme 1 indicate that different substrate binding pathways are followed in the presence of different relative amounts of the substrates, assuming non-rapid-equilibrium conditions.

The MgATP saturation results for the mutant GV212 enzyme (Figure 4) indicate that the substrate inhibition is not due to MgATP binding in the effector site. Thus, inhibition by MgATP occurs as a result of its binding in the active site. Within this context, there are several possible mechanisms by which MgATP inhibition can occur: (1) binding of MgATP to the binary product complex E–Fru-1,6BP to form a dead-end ternary complex E–Fru-1,6BP–MgATP, from which Fru-1,6BP dissociates more slowly than it does from the normal product ternary complex [inhibition of liver alcohol dehydrogenase by ethanol occurs *via* a similar mechanism (Dalziel & Dickinson, 1966)], (2) abortive binding of MgATP in the Fru-6P site (linear substrate inhibition; Cleland, 1979), or (3) the existence of two alternative pathways to the reactive ternary complex, with one pathway kinetically favored (Dalziel, 1957; Ferdinand, 1966). In this last mechanism, inhibition by MgATP would result from the binding of substrates *via* the disfavored pathway.

A mechanism for MgATP inhibition that involves formation of a dead-end complex E–Fru-1,6BP–MgATP is shown to be unlikely from the results of product inhibition studies. Specifically, inhibition by MgATP with respect to Fru-1,6BP in the reverse direction (Table 1) indicates that the complex E–Fru-1,6BP–MgATP does not form readily.

The results of the dead-end inhibition studies in the forward direction using AMPPNP (Table 3 and Figure 5) give evidence for abortive binding of AMPPNP, and presumably ATP, in the Fru-6P site via their γ-phosphate groups. Such abortive binding at least partially explains the observed inhibition by MgATP. However, the experimental evidence suggests that this is not the only mechanism involved.

Dalziel (1957) has shown that substrate inhibition (and activation) are inherent in an alternative-pathways mechanism when the binding or release of substrates is rate-limiting and the rate constants for the steps involved are such that one of the two pathways is kinetically disfavored. Ferdinand (1966) presented the theoretical basis (eq 4) for this mechanism, which can give rise to a variety of nonhyperbolic initial velocity curves (Segel, 1975b), the shapes of which depend on the relative magnitudes of the rate constants for the steps of the mechanism. There is evidence that BsPFK obeys such a mechanism: (1) The binding of MgATP is clearly rate-limiting when its concentration is low, i.e., when it is less than about 3 times the Fru-6P concentration. This indicates that catalysis is fast relative to the rate of MgATP binding. (2) The observed substrate inhibition by MgATP when its concentration is greater than 10-fold the Fru-6P concentration (Figures 2B and 3) is consistent with the binding of substrates through a kinetically disfavored pathway when MgATP concentration is relatively high. Thus, the upper binding pathway in Scheme 1, with MgATP binding first and Fru-6P binding second, is the disfavored pathway for BsPFK. (3) The initial velocity equation for the alternative-pathways mechanism (eq 4) fits the Fru-6P saturation data well (R^2 is 1.000 for the upper curve in Figure 2A) with the assumption that $im \cong jl$ and $ki < mj$,[3] and it fits the MgATP saturation data well (R^2 values are 0.998 and 0.984 for the curves in Figure 3) with the assumption that $im < jl$ and $ki < mj$. Thus, a steady-state alternative-pathways mechanism is consistent not only with the observed substrate inhibition by MgATP but also with other aspects of BsPFK kinetic behavior in the forward direction.

Altogether, the results discussed above provide evidence that BsPFK in the reverse direction obeys a rapid-equilibrium random mechanism. In the forward direction, it obeys an alternative-pathways kinetic mechanism that involves (1) non-rapid-equilibrium binding of MgATP ($k_1, k_6 \ll k_9$ in Scheme 1), evident when MgATP concentration is low, and (2) substrate binding through a kinetically disfavored pathway (the upper pathway in Scheme 1), evident when MgATP concentration is high. In addition, abortive binding of the γ-phosphate of ATP in the Fru-6P site contributes to some extent to the inhibition seen at high MgATP concentration. As such, the kinetic mechanism of BsPFK shares features in common with the kinetic mechanisms of other PFKs, including those from rabbit muscle, *Ascaris suum*, and *E. coli*. Using initial velocity, product inhibition and dead-end inhibition studies, Bar-Tana and Cleland (1974a,b) have shown that the kinetic mechanism of rabbit muscle PFK is sequential random, being rapid-equilibrium in the reverse direction but not in the forward direction, where the rate constants for the release of substrates are lower than the catalytic constant. Although the kinetic mechanism of *A. suum* PFK in the forward direction is predominantly steady-state ordered (Rao *et al.*, 1987), it nevertheless involves some randomness in the order of substrate binding. In the reverse direction, the mechanism is essentially rapid-equilibrium random.

Studies by Deville-Bonne *et al.* (1991a) have indicated that the kinetic mechanism of EcPFK is sequential random and that the binding of one substrate antagonizes the binding of the other. Johnson and Reinhart (1992) have further studied the interactions between MgATP and Fru-6P in the active site of EcPFK by thermodynamic linked-function analysis. Their results indicate that all the observed features of substrate interaction can be explained by two independent couplings: an antagonistic MgATP/Fru-6P coupling extending between active sites and a MgATP-induced Fru-6P/Fru-6P coupling. Zheng and Kemp (1992) have recently proposed that ATP

[3] Substrate activation can be observed in a steady-state alternative-pathways mechanism. Typically, this activation is evident as sigmoidicity in saturation curves with respect to the first substrate to bind the enzyme in the kinetically favored pathway. However, whether or not activation (hence, sigmoidicity) is observed depends on the various rate constants involved and the extent to which one pathway is kinetically favored (or disfavored). Thus, the reason sigmoidicity is not observed in the Fru-6P saturation curve for BsPFK is probably because the extent to which the lower pathway in Scheme 1 is favored (or the upper pathway is disfavored) is not great.

inhibition of EcPFK involves substrate antagonism coupled with a steady-state random mechanism in which the rate of catalysis is too high to permit rapid equilibration of substrates. It is interesting to note that the kinetic behavior of 3-deoxy-D-*arabino*-heptulosonate 7-phosphate synthetase from *Rhodomicrobium vannielii*, which is proposed to follow an alternative-pathways mechanism (Jensen & Trentini, 1970), closely resembles that of EcPFK (Zheng & Kemp, 1992).

Despite similarities between the kinetic mechanisms of EcPFK and BsPFK, the mechanisms by which MgATP inhibits the two enzymes are clearly different. Specifically, MgATP inhibition appears to be allosteric for EcPFK (Berger & Evans, 1991) but not for BsPFK. The reason for this difference has only recently begun to be understood. Steady-state fluorescence studies show that MgATP and Fru-6P each bind to EcPFK noncooperatively in the absence of the other (Deville-Bonne & Garel, 1992). In these studies, cooperative Fru-6P binding was induced by the presence of AMPPCP (and presumably ATP), although the Hill coefficient for the cooperative binding was not as high as that observed in steady-state kinetic measurements (2.0 *versus* 3.8–4.0). Based on studies showing that both k_{cat} and n (the Hill coefficient) vary with pH, Deville-Bonne *et al.* (1991b) have suggested that catalysis and cooperativity are linked in EcPFK. Thus, it is the superimposition of (1) "kinetic cooperativity" resulting from nonequilibrium conditions and (2) concerted binding cooperativity (Monod *et al.*, 1965) that fully explains the allosteric behavior of EcPFK.

The lack of allosteric regulation of BsPFK by MgATP suggests that, unlike EcPFK, catalysis and cooperative Fru-6P binding are not linked. Cooperative binding of Fru-6P does occur, but only in the presence of PEP. The data presented in this paper indicate that MgATP inhibition of BsPFK occurs entirely within the active site by means of (1) abortive MgATP binding and (2) reaction flux through the kinetically disfavored substrate binding pathway. Thus, inhibition of BsPFK by MgATP is a process distinct from allosteric inhibition by PEP.

Finally, the nature of the regulation by MgATP and PEP of BsPFK is compatible with the thermostability of the enzyme. Large conformational changes, which could lead to structural destabilization, are apparently not part of the response of the enzyme to inhibitors. The allosteric transition (Schirmer & Evans, 1990) involves minimal movement: a rotation by 7° of one pair of rigid dimers relative to the other, along with a coordinated back-and-forth movement of a pair of loops (the 8H and 6F loops) across the dimer–dimer interface. Likewise, inhibition by ATP apparently involves little if any conformational change.

ACKNOWLEDGMENT

The authors would like to thank Drs. Paul F. Cook and Alan V. Klotz for helpful discussions during the preparation of the manuscript. We dedicate this work to the memory of David W. H. Chang (1971–1991), son of Dr. S. H. Chang.

REFERENCES

Bar-Tana, J., & Cleland, W. W. (1974a) *J. Biol. Chem. 249*, 1263–1270.

Bar-Tana, J., & Cleland, W. W. (1974b) *J. Biol. Chem. 249*, 1271–1276.

Berger, S. A., & Evans, P. R. (1991) *Biochemistry 30*, 8477–8480.

Blangy, D., Buc, H., & Monod, J. (1968) *J. Mol. Biol. 31*, 13–35.

Cleland, W. W. (1963) *Biochim. Biophys. Acta 67*, 104–137.

Cleland, W. W. (1979) *Methods Enzymol. 63*, 103–138.

Dalziel, K. (1957) *Acta Chem. Scand. 11*, 1706–1723.

Dalziel, K., & Dickinson, F. M. (1966) *Biochem. J. 100*, 34–46.

Deville-Bonne, D., & Garel, J. R. (1992) *Biochemistry 31*, 1695–1700.

Deville-Bonne, D., Laine, R., & Garel, J. R. (1991a) *FEBS Lett. 290*, 173–176.

Deville-Bonne, D., Bourgain, F., & Garel, J. R. (1991b) *Biochemistry 30*, 5750–5754.

Dixon, M., & Webb, E. C. (1979) *Enzymes*, 3rd ed., pp 105–109, Academic Press, New York.

Evans, P. R., Farrants, G. W., & Hudson, P. J. (1981) *Philos. Trans. R. Soc. London B 293*, 53–62.

Ferdinand, W. (1966) *Biochem. J. 98*, 278–283.

French, B. A., & Chang, S. H. (1987) *Gene 54*, 65–71.

Hanson, R. L., Rudolph, F. B., & Lardy, H. A. (1973) *J. Biol. Chem. 248*, 7852–7859.

Hellinga, H. W., & Evans, P. R. (1987) *Nature 327*, 437–439.

Jensen, R. A., & Trentini, W. C. (1970) *J. Biol. Chem. 245*, 2018–2022.

Johnson, J. L., & Reinhart, G. D. (1992) *Biochemistry 31*, 11510–11518.

Larsen, M., Willett, R., & Yount, R. G. (1969) *Science 166*, 1510–1511.

Monod, J., Wyman, J., & Changeux, J. P. (1965) *J. Mol. Biol. 3*, 318–356.

Rao, G. S. J., Harris, B. G., & Cook, P. F. (1987) *J. Biol. Chem. 262*, 14074–14079.

Schirmer, T., & Evans, P. R. (1990) *Nature 343*, 140–145.

Segel, I. H. (1975a) *Enzyme Kinetics*, pp 309–320 and 818–826, John Wiley & Sons, New York.

Segel, I. H. (1975b) *Enzyme Kinetics*, pp 657–659, John Wiley & Sons, New York.

Shirakihara, Y., & Evans, P. R. (1988) *J. Mol. Biol. 204*, 973–994.

Valdez, B. C., French, B. A., Younathan, E. S., & Chang, S. H. (1989) *J. Biol. Chem. 264*, 131–135.

Yoshida, M. (1972) *Biochemistry 11*, 1087–1093.

Yount, R. G., Babcock, D., Ballantyne, W., & Ojala, D. (1971) *Biochemistry 10*, 2484–2489.

Zheng, R. L., & Kemp, R. G. (1992) *J. Biol. Chem. 267*, 23640–23645.